

Theoretical Model for the Nanobundle Network Transistors Below and Above Percolation Limit

Ninad Pimparkar ^{a*}, Jing Guo ^b and M. A. Alam ^a

^a School of Electrical and Computer Engineering, Purdue University, West Lafayette, IN 47907, USA.

^b Department of Electrical and Computer Engineering, University of Florida, Gainesville, Florida 32611 USA.

*Phone: (765) 494 9034 Fax: (765) 494 6441 Email: ninad@purdue.edu.

ABSTRACT

Nanobundle network transistors (NBTs) have emerged as a viable, higher performance alternative to poly-silicon and organic transistors with possible applications in macroelectronic displays, chemical/biological sensors, and photovoltaics. A simple analytical model for I-V characteristics of NBTs (below the percolation limit) and a numerical model (above the percolation limit) is proposed. The physics-based predictive model provides a simple relation between transistor characteristics and design parameters which can be used for optimization of NBTs.

Keywords: Carbon Nanotube, Stick Percolation, Network Transistor, Inhomogeneous Percolation Theory, Thin Film Transistor.

1 INTRODUCTION

Recently there have been a number of reports regarding a new class of thin film transistors based on percolating network of randomly-oriented, finite-length Silicon nanowires (NW) and Carbon nanotubes (NT) [1-6], as shown in Fig. 1. At densities below the percolation limit ($\rho < \rho_{TH}$ [7]), the transistors may have applications in microelectronics and power transistors with on-current (I_{ON}) of the order of milliamps, much higher than a single NW/NT devices but still with on/off ratio ~ 500 [1]. For NT/NW densities above the percolation limit ($\rho > \rho_{TH}$), NBTs have emerged as a viable, higher performance alternative to poly-silicon[8] and organic transistors[9] with possible applications in macroelectronic displays, chemical/biological sensors, photovoltaics[1-6]. Several groups have reported a wide variety of experimental data,

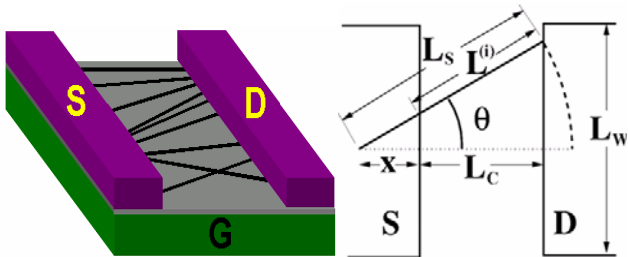


Fig. 1 Geometry of nanobundle network transistor: (a) A schematic of NBT. (b) A nano-stick between the S/D electrodes making an angle θ with the channel axis.

but there is no unifying theoretical model to explain these recent experiments. In this paper, we propose and validate a simple theory of I-V characteristics of NBTs (below and above the percolation threshold) and use the theory to model recent experiments and assess device performance.

2 FOR NBT BELOW PERCOLATION THRESHOLD

2.1 Analytical Model

Consider a typical NBT[1, 10] (Fig. 1a) assembled with a bundle of nano-sticks of length L_s , isotropically oriented ($0 \leq \theta < 2\pi$) onto gate oxide surface. L_c , L_w , $L^{(i)}$ and x (Fig. 1b) are channel length, channel width, intercepted channel length for individual sticks and total stick overlap component with the S/D along channel axis, respectively. For $L_c < L_s$ and $\rho < \rho_{TH}$, the tube-tube interaction is unimportant. Assuming uniform probability of germination at all locations, the number of sticks bridging S/D and making an angle between θ and $\theta + d\theta$ with the channel axis (Fig. 1b and Fig. 2) is given by,

$$dN_s(\theta) = (D_c \cdot x) d\theta / (\pi/2) = (2D_c / \pi)(L_s \cos\theta - L_c) d\theta$$

where, D_c is linear tube density and $\cos\theta = (L_c + x) / L_s$.

Total number of sticks bridging S/D, N_s , is given by summing over all the angles from θ to $\theta_{max} = \cos^{-1} L_c / L_s$. Therefore,

$$N_s(R_s) = 2D_c L_s / \pi g_B(R_s)$$

where $R_s = L_c / L_s$, and $g_B(y) = (1 - y^2)^{1/2} - y \cos^{-1} y$.

Ballistic limit: For NBTs in short channel limit all the sticks are in ballistic limit and the current is given by,

$$I_B = L_w C_{ox} [V_G - V_{TH}] v_T N_s \quad (1)$$

where $v_T = (2K_B T / \pi m^*)^{1/2}$ is thermal velocity, V_{TH} is threshold voltage and C_{ox} is gate capacitance. The ballistic current is proportional to number of sticks, as expected.

Velocity saturation limit: For NBTs in high bias all the sticks can be in velocity saturation limit so that magnitude of current is independent of individual stick length. Therefore overall transport is again independent of channel length and,

$$I_{sat} = L_w C_{ox} [V_G - V_{TH} - V_D / 2] v_{sat} N_s \quad (2)$$

where v_{sat} is saturation velocity of the carriers.

Long channel limit: For NBTs with longer channel limit, the transport in each of the bridging sticks is diffusive and is inversely proportional to intercepted channel length, $L^{(i)}$, for each stick. The current is given by,

$$\frac{I_D}{f(V_D, V_G)} = \int_0^{\theta_s} \frac{2D_c L_c b (L_s \cos \theta - L_c)}{\pi L_c / \cos \theta} d\theta = \frac{D_c}{\pi} g_D(R_S) \quad (3)$$

where $g_D(y) = \cos^{-1} y / y - (1 - y^2)^{1/2}$, $\theta_s = \cos^{-1} R_S$ and $f(V_D, V_G) = \mu_0 L_W C_{OX} [(V_G - V_{TH}) V_D - \beta V_D^2]$ [11].

Finally, for the intermediate channel lengths, the sticks parallel to channel axis, $\theta \sim 0$, are near ballistic limit and sticks making an angle, $\theta \sim \theta_{max}$, with channel axis are near

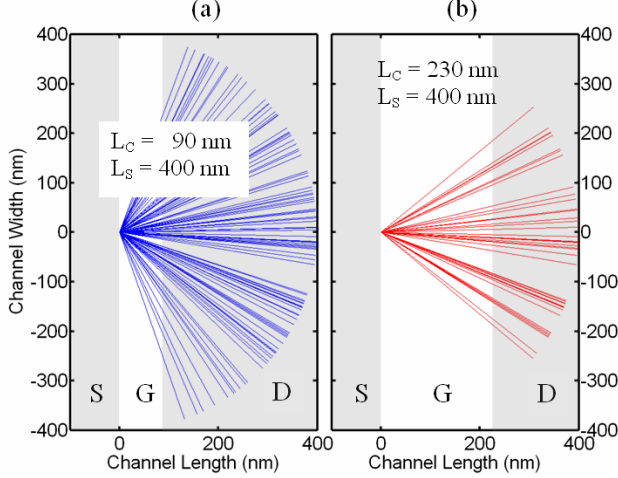


Fig. 2 *Fan Diagram*: If all sticks in Fig. 1a were collected at a point (with angles preserved), it is easy to see that more sticks connect S/D for a transistor with a shorter channel length. Here, stick length is $L_S = 400$ nm and channel lengths are (a) $L_C = 90$ nm and (b) $L_C = 230$ nm.

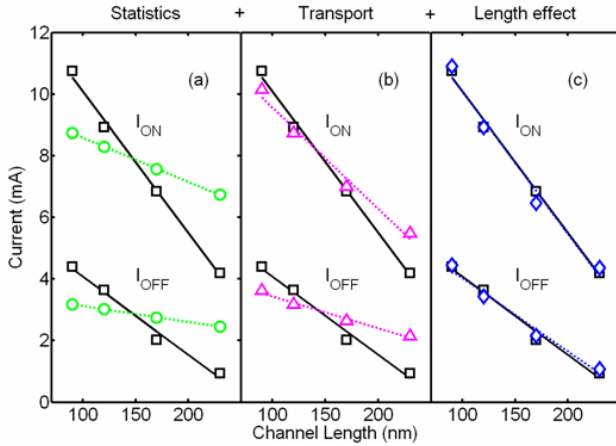


Fig. 3 Experimental [1] (squares with solid line fit) and theoretical (dotted line fits) I_{ON} and I_{OFF} vs. L_C . The inverse scaling of I_{ON} and I_{OFF} with L_C is a consequence of sequential addition of (a) *Statistical effect*: Increased probability of sticks to bridge S/D as channel length decreases (Fig 2), (b) *Transport effect*: Prevalence of ballistic transport in shorter channel devices, and (c) *Average length effect*: Average length for m-SWCNT $\langle L_M \rangle \sim 350$ nm is made less than s-SWCNTs $\langle L_S \rangle \sim 1000$ nm. Here, mean free path for s-SWCNT $\lambda_D \sim 200$ nm. Note that theory matches well with experiment only after all three effects are included in the simulation as shown in (c).

diffusive limit. And the proportion of the two types of sticks changes with applied bias. Still, the I-V characteristics of any single nanostick can be described by a simple analytical expression based on a transmission point of view [12]. An exact analytical result for NBTs can be obtained by replacing $1/L^{(i)}$ with $1/(L^{(i)} + \lambda)$ where $\lambda = \min(\lambda_D, \lambda_{sat} = V_D \mu_0 / v_{sat})$ and λ_D is the mean free path for carriers. Hence, the total current

$$\frac{I_T}{f(V_G, V_D)} = \int_0^{\theta_s} \left(\frac{2D_c}{\pi} \frac{L_s \cos \theta - L_c}{L_c / \cos \theta + L_c b} \right) d\theta \quad (4)$$

$$= \frac{2D_c}{\pi b^2} \left[b g_B(R_S) - \cos^{-1} R_S + \frac{2(b R_S + 1)}{\sqrt{b^2 - 1}} \tanh^{-1} \frac{(b-1) \tan(\theta_s / 2)}{\sqrt{b^2 - 1}} \right]$$

where, $b = \lambda / L_C$ (Fig. 2a). As $\lambda \rightarrow 0$, $I_T \rightarrow I_D$, and as $\lambda \rightarrow \infty$, $I_T \rightarrow I_{sat}$.

2.2 Discussion

The model helps explain the inverse scaling of I_{ON} vs. L_C and I_{OFF} vs. L_C (Fig. 3) in the recent measurements of CNT-NBTs [1] as a combination of three factors associated with random distribution of tubes: (1) *Statistical effect*: Increased probability of sticks to bridge S/D as channel length decreases (Fig. 2, 3a), (2) *Transport effect*: Prevalence of ballistic transport in shorter channel devices (Fig. 3b), and (3) *Average length effect*: Average length for metallic (m)-SWCNT $\langle L_M \rangle \sim 350$ nm being less than semiconducting (s)-SWCNTs $\langle L_S \rangle \sim 1000$ nm (Fig. 3c). Fig. 5d and 5e show the relative contribution from the three effects. The total statistical effect, which is sum of (1) and (3), plays a dominant role in interpreting this experiment. Here, mean free path for s-SWCNT $\lambda_D \sim 200$ nm.

3 FOR NBT ABOVE PERCOLATION THRESHOLD

3.1 Numerical Model

For NBTs with $L_C > L_S$ and density higher than percolation threshold (Fig 4a) the stick-stick interaction is important and analytical solution is not possible. Therefore, $n(V_D, V_G)$ must be determined self-consistently by solving the drift-diffusion equations (appropriate for $L_C > 1 \mu\text{m}$) and the Poisson equation which are generalized for NBT as:

$$\left. \begin{aligned} \frac{d^2 \Phi}{ds^2} + \frac{\rho}{\epsilon} &= 0 \\ \nabla \cdot J_p &= 0 \\ \nabla \cdot J_n &= 0 \end{aligned} \right\} \rightarrow \left. \begin{aligned} \sum_{i=1}^N \left(\frac{d^2 \Phi_i}{ds^2} + \frac{\rho_i}{\epsilon} - \frac{(\Phi_i - V_G)}{\lambda^2} + \sum_{j=1}^N \frac{(\Phi_j - \Phi_i)}{\lambda_{ij}^2} \right) &= 0, \\ \sum_i \left(\nabla \cdot J_{pi} + \sum_{j=1}^N C_{ij}^p (p_j - p_i) \right) &= 0, \\ \sum_i \left(\nabla \cdot J_{ni} + \sum_{j=1}^N C_{ij}^n (n_j - n_i) \right) &= 0, \end{aligned} \right\} \quad (5)$$

where, N is total number of NT/NW, s is in the direction of individual NW/NT, $\rho(x, y)$ is total charge density, and the term $-(\Phi - V_G) / \lambda^2$ (the well known parabolic approximation [13, 14]) introduces the effect of back gate, where λ is effective screening length. The term $(\Phi_j - \Phi_i) / \lambda_{ij}^2$ is stick-stick interaction with screening length λ_{ij} where a node on

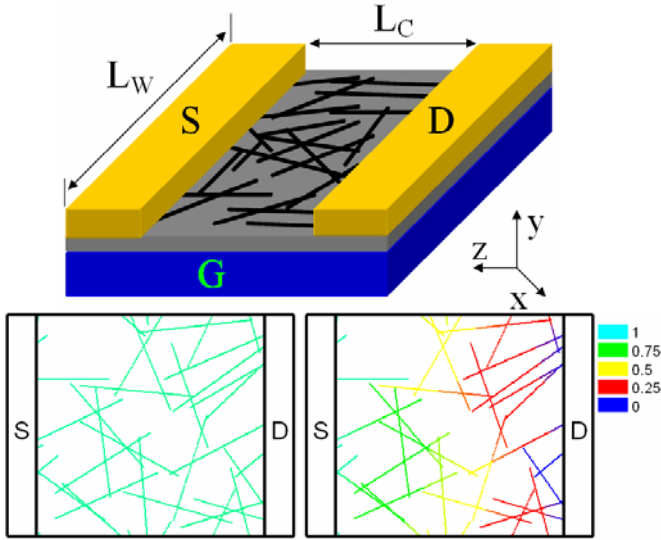


Fig. 4. (a) A schematic of NBT: Geometry of nanobundle network transistor. Distribution of normalized conductance along the sticks in the random network in (b) low and (c) high bias, respectively. The conductance is uniform along the channel in low bias while it varies nonlinearly in the high bias condition resulting in an inhomogeneous percolating network and the contours of conductance are not straight lines parallel to S/D as in conventional MOSFET.

stick i intersects a node on stick j . The intersecting nodes act as tiny gates for each other modifying the potential and carrier concentrations [15]. Further, transport is essentially 1D (along the tube) with the additional term $C_{ij}^{n,p}$ ($n_j - n_i$) in the continuity equation representing charge transfer between nanosticks at the point of intersection. Here higher value of $C_{ij}^{n,p} = G_0/G_1$ implies better electrical contact, where G_0 and G_1 is mutual and self conductances of the tubes [16].

Doped S/D contacts [17] are assumed to simulate NBT using the Eq. (5) and the initial guess is the equilibrium solution. An iterative self consistent solution is found using Scharfetter-Gummel method of discretization [18]. In each of the iterations, an array, k , is filled with 3 elements (corresponding to 3 unknowns Φ , n , and p) for each node on all the tube with the current solution substituted into LHS of the Eq. (5). If the tube is touching S/D contacts a constant potential boundary condition is imposed otherwise a floating boundary condition is imposed. Then a 2-D sparse derivative matrix, J , is populated with mostly lower sub-diagonal entries except a few off-diagonal terms corresponding to the tube-tube interaction. Finally, at the end of each iteration, the correction to potential and charge distribution is obtained as, $dk = J^{-1} k$ and the simulation is stopped when correction to each node is below a threshold value.

3.2 Discussion

It was shown in section 2 above that in the ‘short-channel limit of $L_C < L_S$ and at low stick density, the

NW/NTs behave as individual transistors connected in parallel and therefore the ratio of the I_D for any two bias points is independent of the geometry of the NB-TFTs. For $L_C > L_S$ the numerical simulations [19] show that the scaling relationship is still valid and current can be written as

$$I_D = \frac{A}{L_S} \xi \left(\frac{L_S}{L_C}, \rho_s L_S^2 \right) \times f(V_G, V_D), \quad (6)$$

where the proportionally constant A depends on oxide capacitance C_{ox} , tube diameter d [20], and stick-stick interaction parameter, $C_{ij}^{n,p}$. And ξ and f are functions of geometrical parameters (L_S , L_C , ρ_s) and bias conditions (V_D , V_G), respectively. We find that the geometrical factor ξ can be written as

$$\xi \left(\frac{L_S}{L_C}, \rho_s L_S^2 \right) = \left(\frac{L_S}{L_C} \right)^{m(\rho_s L_S^2)} \quad (7)$$

where m is a universal exponent of stick percolating system. Fig. 5(a) shows the I_D - V_D characteristics of two different random networks for $V_G - V_{TH} = 1.0$ V, $L_S = 1$ μ m and $L_W = 200$ μ m. Fig 5(b) compares the current vs. normalized channel length characteristics from the analytical ($L_C/L_S < 1$) and numerical ($L_C/L_S > 1$) models. The analytical model ignores tube-tube interaction and is only valid for $L_C/L_S \ll 1$, while the numerical model assumes that the current through each tube is limited by diffusive transport and hence is only valid for $L_C \gg \lambda$, the mean free path for the carriers.

For densities much higher than percolation threshold ($\rho_s L_S^2 \gg \rho_{th} = 4.236^2/\pi$ [7]), the network behaves as a 2D conductor with $m = 1$. Together with Eq. (7) below we find that Eq. (6) reduces to the classic ‘square law’ as expected. But for densities near percolation threshold ($\rho_s L_S^2 \sim 4.236^2/\pi$) the exponent takes the value $m \sim 1.8$ (Fig. 5b). Moreover, Fig. 5a shows that the bias-dependent scaling

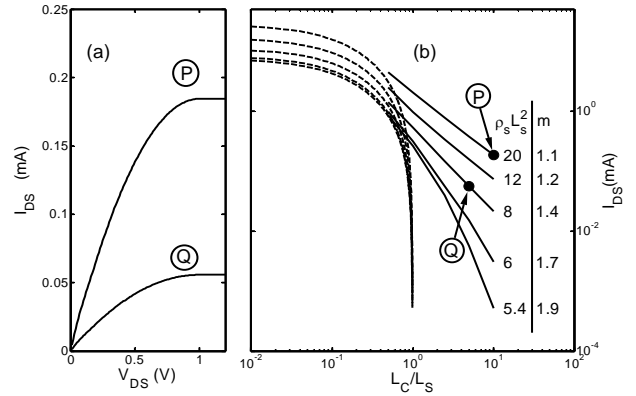


Fig. 5: (a) The source-drain current vs. V_{DS} for $V_G - V_{TH} = 1.0$ V for two networks P and Q with different densities and L_C (as shown in b) here, $L_S = 1$ μ m and $L_W = 200$ μ m. (b) The on-current vs. normalized channel length computed by analytical model for $L_C < L_S$ (Eq. 4, dotted curves) and numerical model (Eq. 6, solid lines) for $V_G - V_{TH} = 1.0$ V and $V_D = 1$ V.

function

$$f(V_G, V_D) = [(V_G - V_{TH})V_D - \beta V_D^2] \quad (8)$$

is independent of geometrical parameters ($\beta \sim 0.5$), again satisfying Eq. (6). At very low densities ($\rho \ll \rho_{th}$), where system behaves as an independent collection of 1D (long-channel) conductors and at very high densities ($\rho \gg \rho_{th}$), where the percolating network approximates a classical 2D homogenous thin film limit, the voltage scaling function $f(V_G, V_D)$ would follow the classical ‘square-law’ formula. But, for $\rho \sim \rho_{th}$, the constant conductivity contours in high bias regime may not be the lines perpendicular to channel axis (Fig. 4b), linear percolation theory may not be applicable and a classical MOSFET like behavior may not be expected. But surprisingly, our simulations show that Eq. (6) holds for arbitrary stick density above and below the percolation threshold. This robust density independent voltage scaling may be arising from the fact that, given the 1D approximation to Poisson equation in (1), any random network of sticks can be reduced to a single (homogeneous) thin-film strip of effective width W .

The implication of our results is that once A , V_{TH} and β is determined (for Eq. 6) by I_D - V_D and I_D - V_G measurement and m is determined from Fig. (5b) for particular L_S , L_C , and ρ_S for one of the transistors, one can readily determine the transistor performance of any other transistor of arbitrary L_S , L_C , and ρ_S , (Fig. 5b) and biasing condition reducing the technology development and characterization time significantly. Second, Eq. (6) provides a ‘bottom-up’ definition of effective-mobility, $\mu_{eff} \sim (dI_D/dV_G/V_D) (L_S/\xi) / (L_W C_{OX})$, the value of which is independent of L_C and can be used to compare experimental data from various laboratories. For very high density networks, μ_{eff} reduces to conventional mobility equation as $m = 1$ and $\xi = L_S/L_C$ in Eq. (7).

4 CONCLUSIONS

We have proposed a simple analytical model for I-V characteristics of NBTs (below the percolation limit) and a numerical model (above the percolation limit). We have generalized the linear stick percolation theory to nonlinear regime to find a scaling formula (6) to compute I_D - V_D characteristics of NB-TFT that, once calibrated, can be used to establish performance limits of NB-TFTs of arbitrary geometry and operating conditions. Our analysis therefore would help organize experimental data from various research groups and could have significant impact on the development of NB-TFT technology.

ACKNOWLEDGEMENTS

This work was supported by the Network of Computational Nanotechnology and the Lilly Foundation. The authors would like to thank Prof. J. Rogers, Prof. J. Y. Murthy, C. Kocabas and S. Kumar for many valuable discussions.

REFERENCES

- [1] R. Seidel, A. P. Graham, E. Unger, G. S. Duesberg, M. Liebau, W. Steinhoeagl, F. Kreupl, and W. Hoenlein, *Nano Lett.*, vol. 4, pp. 831-834, 2004.
- [2] X. F. Duan, C. M. Niu, V. Sahi, J. Chen, J. W. Parce, S. Empedocles, and J. L. Goldman, *Nature*, vol. 425, pp. 274-278, 2003.
- [3] E. S. Snow, J. P. Novak, P. M. Campbell, and D. Park, *Appl. Phys. Lett.*, vol. 82, pp. 2145-2147, 2003.
- [4] E. S. Snow, J. P. Novak, M. D. Lay, E. H. Houser, F. K. Perkins, and P. M. Campbell, *J. of Vac. Sci. and Tech. B*, vol. 22, pp. 1990-1994, 2004.
- [5] Y. X. Zhou, A. Gaur, S. H. Hur, C. Kocabas, M. A. Meitl, M. Shim, and J. A. Rogers, *Nano Lett.*, vol. 4, pp. 2031-2035, 2004.
- [6] E. Menard, K. J. Lee, D. Y. Khang, R. G. Nuzzo, and J. A. Rogers, *Appl. Phys. Lett.*, vol. 84, pp. 5398-5400, 2004.
- [7] G. E. Pike and C. H. Seager, *Phys. Rev. B*, vol. 10, pp. 1421-1434, 1974.
- [8] C. R. Kagan and P. Andry, vol. New York: Marcel Dekker, 2003.
- [9] C. D. Dimitrakopoulos and D. J. Masecaro, *IBM J. of Res. And Dev.*, vol. 45, pp. 11-27, 2001.
- [10] N. Pimparkar, J. Guo, and M. A. Alam, "Performance Assessment of Sub-Percolating Nanobundle Network Transistors by an Analytical Model," presented at IEDM Tech. Digest, 2005.
- [11] Y. Taur and T. Ning, vol.: Cambridge Univ. Press, 1998.
- [12] J. Wang and M. Lundstrom, *IEEE Trans. on Elect. Dev.*, vol. 50, pp. 1604-1609, 2003.
- [13] K. K. Young, *IEEE Trans. on Elect. Dev.*, vol. 36, pp. 399-402, 1989.
- [14] F. G. Pikus and K. K. Likharev, *Appl. Phys. Lett.*, vol. 71, pp. 3661-3663, 1997.
- [15] M. S. Fuhrer, J. Nygard, L. Shih, M. Forero, Y. G. Yoon, M. S. C. Mazzoni, H. J. Choi, J. Ihm, S. G. Louie, A. Zettl, and P. L. McEuen, *Science*, vol. 288, pp. 494-497, 2000.
- [16] S. Kumar, J. Y. Murthy, and M. A. Alam, *Phys. Rev. Lett.*, vol. 95, 2005.
- [17] A. Javey, R. Tu, D. B. Farmer, J. Guo, R. G. Gordon, and H. J. Dai, *Nano Lett.*, vol. 5, pp. 345-348, 2005.
- [18] R. W. Dutton and Z. Yu, vol. Boston: Kluwer Academic Publishers, 1993.
- [19] N. Pimparkar, S. Kumar, J. Y. Murthy, and M. A. Alam, Submitted to *Elect. Dev. Lett.*, 2006.
- [20] X. J. Zhou, J. Y. Park, S. M. Huang, J. Liu, and P. L. McEuen, *Phys. Rev. Lett.*, vol. 95, 2005.